www.elsevier.nl/locate/jorganchem

Journal of Organometallic Chemistry 584 (1999) 103–117

Journal of Organometallic Chemistry

# Mono-aryltin(IV) and mono-benzyltin(IV) complexes with pyridine-2-carboxylic acid and 8-hydroxyquinoline. X-ray structure of *p*-chloro-phenyl-tris(8-quinolinato)tin(IV)·$2CHCl_3$

Markus Schürmann [a], Ralf Schmiedgen [a], Friedo Huber [a,*], Arturo Silvestri [b], Giuseppe Ruisi [b], Adriana Barbieri Paulsen [c], Renato Barbieri [b]

[a] *Fachbereich Chemie, Universität Dortmund, Otto-Hahn Str. 6, D-44221 Dortmund, Germany*
[b] *Dipartimento di Chimica Inorganica, Università di Palermo, viale delle Scienze, I-90128 Palermo, Italy*
[c] *Institut für Physik, Medizinische Universität Lübeck, Ratzeburger Allee 160, D-23538 Lübeck, Germany*

Received 30 October 1998; received in revised form 17 December 1998

---

## Abstract

Complexes $RSn(O_2CPy)_3 \cdot 2H_2O$ and $RSn(Ox)_3$, (PyCOOH = pyridine-2-carboxylic acid, HOx = 8-hydroxyquinoline, R = *o*- and *p*-Tolyl, *o*- and *p*-$ClC_6H_4$ = *o*- and *p*-ClPh, o-$ClC_6H_4CH_2$ = *o*-ClBenzyl; besides, R = Ph in $RSn(Ox)_3$) have been synthesized and characterized by elemental analysis and determination of molecular weights in $CHCl_3$ solutions. The structure of *p*-ClPh-$Sn(Ox)_3 \cdot 2CHCl_3$ has been determined by X-ray diffractometry. The 7-coordinated tin atom of the monomeric compound is in the center of a pentagonal bipyramid formed by (*p*-ClPh)C and O and N atoms of the chelating $Ox^-$ ligands. The latter type of structure would hold for all complexes according to $^{119}Sn$ Mössbauer (including the determination of the dynamics of $^{119}Sn$ nuclei) and IR spectroscopy in the solid state; the ligand $^-O_2CPy$ appears to chelate Sn through one oxygen atom of the $-COO^-$ group and the N atom, although the occurrence of one chelating and two monodentate $PyCO_2^-$ ligands (through $-COO^-$), and coordination by the $H_2O$ molecules to Sn cannot be excluded. In $CDCl_3$ and $CHCl_3$ solutions, the persistence of the pentagonal bipyramidal species is assumed, in line with $^1H$-, $^{13}C$-, $^{119}Sn$-NMR and UV–vis spectroscopic studies. © 1999 Elsevier Science S.A. All rights reserved.

*Keywords:* Tin; Pyridyl-2-carboxylic acid; 8-Hydroxyquinoline; X-ray structure

---

## 1. Introduction

In a preceding paper, we reported the synthesis and characterization of mono-organotin(IV) complexes $RSnCl_2(L)$, $RSnCl(L)_2$ and $RSn(L)_3$ (HL = 2-mercapto-pyridine = HSPy, and 2-mercapto-pyrimidine = HSPym, R = Alkyl, Ph) by IR and $^{119}Sn$ Mössbauer spectroscopy in the solid state, and $^1H$-, $^{13}C$- and $^{119}Sn$-NMR spectroscopy in solution phases [1]. X-ray diffractometry revealed that in complexes $RSn(SPy)_3$ (R = Me, Ph) bidentate $SPy^-$ ligands and (R)C form a pentagonal bipyramidal polyhedron around tin [1].

Among the $RSn(SPy)_3$ species investigated, organotin(IV) moieties $RSn^{IV}$ with R = *o*-Tolyl, *p*-Tolyl, *o*-ClPh, *p*-ClPh, Benzyl and *o*-ClBenzyl have been taken into account [1], whose coordination chemistry has rarely been studied [2].

Continuing our work in the field, we report here on complex formation of RSn moieties with the ligands pyridine-2-carboxylate ($^-O_2CPy$) and 8-hydroxyquinolinate ($Ox^-$), Fig. 1; complexes $RSn(O_2CPy)_3$ and $RSnOx_3$ have been synthesized, and structurally characterized.

$^-O_2CPy$ (potentially tridentate [3,4]) may act as bidentate ligand, coordinating to metal centers by heterocyclic nitrogen and one oxygen atom of the carboxylic group, and forming chelate rings analogous to those in 8-hydroxyquinolinate complexes; it follows that related compounds are mutually comparable [5]. Besides, bonding and structure in $^-O_2CPy$ and $Ox^-$

---

[*] Corresponding author. Tel.: +49-231-7553801; fax: +49-231-7553797.

PII: S0022-328X(99)00103-5

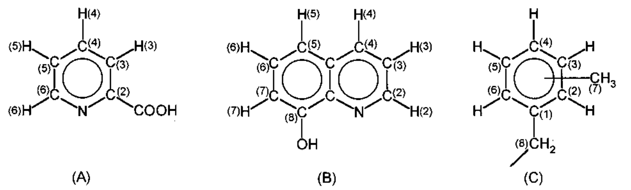

Fig. 1. Ligand molecules, and labelling employed in Tables 8 and 9, NMR data. (A) pyridine-2-carboxylic acid; (B) 8-hydroxyquinoline; (C) organic radicals (benzyl and tolyl) bound to Sn.

complexes may be discussed in connection with the corresponding SPy$^-$ derivatives [6].

The coordination of $^-O_2CPy$ to organotin(IV) acceptors, mainly $R_2Sn^{IV}$ and $R_3Sn^{IV}$, has been previously investigated by X-ray diffractometry [3,4,7,8] as well as by IR, NMR and $^{119}Sn$ Mössbauer spectroscopies [4–6,9–14]. It has been established that the ligand may act as mono-, bi- and tridentate, in the latter case yielding polymeric species through bridging by the carboxylate group [3–14].

Complexes of $R_nSn^{IV}$ ($n = 1–3$) with 8-hydroxyquinoline and related ligands have been widely investigated by X-ray diffractometry [2,15–19], $^{119}Sn$ Mössbauer spectroscopy [6,20–34], IR, NMR, UV–vis and other techniques [6,9,13,19–21,26,33–57]. UV spectra and syntheses have been reported as early as in 1950–1961 [58]. The ligand Ox$^-$ behaves essentially as bidentate in solid state complexes, possibly as monodentate in $R_3SnOx$ in ethanol (aqueous) solution [36,37]; it chelates Sn in $R_3SnOx$ in anhydrous cyclohexane, dioxane and $CCl_4$ solutions [39,53]. In $R_2SnOx_2$, the R radicals and the two chelating Ox$^-$ ligands may lie in cis-position, both in the solid state [2,15,18] and in solution phases [41], as well as in trans-configuration [16]. Ox$^-$ proved to be bidentate in $R_2SnCl(Ox)$ in alcohol and benzene solution [42]. Mono-organotin(IV) complexes $^nBuSnOx_3$ [21,25,28,43], and $EtSnOx_3$ [30] (Ox = 5,7-dichloro-; 5,7-dibromo; 5-nitro-8-oxy-quinolinate [30]), have been determined to consist of pentagonal bipyramidal type species, with 7-coordinated Sn, by $^{119}Sn$ Mössbauer spectroscopy [21,25,28,30], and IR, NMR,UV spectroscopies [43].

## 2. Experimental

### 2.1. Materials

Pyridine-2-carboxylic acid, 8-hydroxyquinoline and $Ph_4Sn$ were products from E. Merck, Darmstadt, and $SnCl_4$ from Th. Goldschmidt A.G., Essen. Other reagents and solvents were commercial products, which were purified and dried according to standard procedures [59].

### 2.2. Syntheses

These were generally effected in dry solvents, under stirring, in dry nitrogen atmosphere. Mono-organotin trichlorides were prepared by the Kozeschkow reaction [60] from $R_4Sn$ and $SnCl_4$ [61]; tetraorganotin(IV) derivatives, R = *o*- and *p*-Tolyl, *o*- and *p*-chlorophenyl, Benzyl and *o*-chloro-Benzyl, were obtained by standard procedures [61].

The complexes $RSn(O_2CPy)_3 \cdot 2H_2O$, **1**–**5** in Table 1, were obtained by reaction of $NaO_2CPy$, in methanol solution, with $RSnCl_3$ in chloroform, by the same procedure employed for the syntheses of $^-SPy$ and $^-SPym$ complexes [1]. The *p*-Tolyl$Sn^{IV}$ derivative, **1** in Table 1, was also obtained from *p*-TolylSn(OOH) [19](a), according to previously reported procedures [1]. Compound **5′** in Table 4, $BzSn(O_2CPy)_3$, was prepared by reaction of a mixture of BzHgCl and $BzSnCl_3$ with $NaO_2CPy$, again following the procedure reported for $^-SPy$, $^-SPym$ complexes [1]; in the present context, attempts to separate the products $BzHg(O_2CPy)$ and $BzSn(O_2CPy)_3$ were unsuccessful.

#### 2.2.1. Complexes $RSnOx_3$ were prepared as follows

(a) Numbers **6**–**10**, Table 1: $RSnCl_3$ (6 mmol) and 1 ml of concentrated $NH_3$ were added to a solution of HOx (24 mmol) in 60 ml MeOH. The mixture was refluxed for 3 h. The obtained solid product was filtered off, washed with MeOH and dried under vacuum in the presence of $P_2O_5$.

(b) Number **11**, Table 1: HOx (21 mmol) was treated with NaOMe (21 mmol, 42 ml of a 0.5 M solution); the obtained solution was added dropwise, within 1 h, to a solution of *o*-ClBz$SnCl_3$ (6 mmol) in 40 ml of absolute MeOH. After stirring (24 h) at r.t., the solvent was removed in a rotary evaporator; the residue was dissolved in 50 ml $CHCl_3$, and NaCl was filtered off. The volume of the solution was reduced to about 20 ml, and petroleum ether (b.p. 30–60°C) was added in small portions till the solution attained a yellowish color. The crystallization of the complex was obtained at $-30$°C; the product was filtered off and dried under vacuum.

### 2.3. Characterization of the complexes

Decomposition temperatures (uncorrected; Table 1) were determined by DTA/TG measurements with a Mettler Vacuum thermoanalyzer T1 (Reference: $Al_2O_3$, 25°C; $N_2$, 6°C min$^{-1}$; Pt/PtRh thermoelement). Molecular weights (Table 1) were measured with a Knauer vapor pressure osmometer on $CHCl_3$ solutions. C, H, N analyses (Table 1) were effected with an Elemental Analyzer 1106, Carlo Erba, or determined at the Dipartimento di Chimica Inorganica, Organometallica ed Analitica, University of Padova (Italy).

Table 1
Analytical data for mono-aryltin(IV) and mono-benzyltin(IV) complexes with pyridine-2-carboxylic acid ($HO_2CPy$) and 8-hydroxyquinoline (HOx)

| Number | Compound [a] | Yield (%) | M.P. (°C) | Mol. wt. found (calc.) [b] | Analytical data: found (calcd.)% | | |
|---|---|---|---|---|---|---|---|
| | | | | | C | H | N |
| **1** | *p*-$TolSn(O_2CPy)_3 \cdot 2H_2O$ | 71 | 256(dec) | 607 (612.2) | 49.1 (49.1) | 3.1 (3.8) | 6.9 (6.9) |
| **2** | *o*-$TolSn(O_2CPy)_3 \cdot 2H_2O$ | 68 | 245(dec) | 585 (612.2) | 48.9 (49.1) | 3.4 (3.8) | 7.0 (6.9) |
| **3** | *p*-$ClPhSn(O_2CPy)_3 \cdot 2H_2O$ | 70 | 267(dec.) | 638 (632.6) | 45.2 (45.6) | 2.9 (3.2) | 6.5 (6.6) |
| **4** | *o*-$ClPhSn(O_2CPy)_3 \cdot 2H_2O$ | 65 | 265(dec) | 633 (632.6) | 45.5 (45.6) | 3.0 (3.2) | 6.6 (6.6) |
| **5** | *o*-$ClBzSn(O_2CPy)_3 \cdot 2H_2O$ | 70 | 240(dec) | 647 (646.6) | 46.3 (46.4) | 3.5 (3.4) | 6.5 (6.5) |
| **6** | $PhSn(Ox)_3$ | 82 | 316(dec) | —(628.2) | 62.8 (63.1) | 3.7 (3.7) | 6.7 (6.7) |
| **7** | *p*-$TolSn(Ox)_3$ | 79 | 249(dec) | —(642.3) | 63.6 (63.6) | 3.9 (3.9) | 6.5 (6.5) |
| **8** | *o*-$TolSn(Ox)_3$ | 78 | 270(dec.) | —(642.3) | 63.4 (63.6) | 4.0 (3.9) | 6.5 (6.5) |
| **9** | *p*-$ClPhSn(Ox)_3$ | 84 | 245(dec) | —(662.7) | 59.3 (59.8) | 3.4 (3.4) | 6.3 (6.4) |
| **10** | *o*-$ClPhSn(Ox)_3$ | 80 | 273(dec) | —(662.7) | 59.6 (59.8) | 3.5 (3.4) | 6.5 (6.4) |
| **11** | *o*-$ClBzSn(Ox)_3 \cdot CHCl_3$ | 74 | 151(dec) | 655(676.7) [c] | 52.7 (52.8) | 3.3 (3.2) | 4.9 (5.3) |

[a] Abbreviations: Tol = Tolyl; Ph = Phenyl; Bz = Benzyl; *o* = ortho; *p* = para.

[b] In $CHCl_3$ solutions. The calculated MW values for Numbers **1**–**5** include $2H_2O$ per mole. Numbers **6**–**10**: MW not determined owing to insufficient solubility.

[c] Molecular mass calculated for *o*-$ClBzSn(Ox)_3$.

Single crystals of *p*-$ClPhSnOx_3 \cdot 2CHCl_3$ were obtained by crystallization from $CHCl_3$, analogously to the procedure in a previous study [1]. Intensity data for the yellow crystals were collected with $\omega/2\vartheta$ scans on a Nicolet R3m/V diffractometer with graphite-monochromated Mo–$K_\alpha$ radiation at 170(1)K. The lattice parameters were determined from a symmetry-constrained least-squares fit of the angular settings for 49 reflections with $2\theta_{max} = 30.4°$. Six standard reflections were recorded every 300 reflections and anisotropic intensity loss up to 2.3% was detected during X-ray exposure. The data were corrected for Lorentz-polarisation decay and for absorption effects. The structure was solved by direct methods using SHELXS86 [62] and successive difference Fourier syntheses. Refinement applied full-matrix least-squares methods (SHELXL93 [63]). The H atoms were placed in geometrically calculated positions and refined with a common isotropic temperature factor ($H_{aryl}$ C–H 0.95 Å, $U_{iso}$ 0.049(4) Å$^2$). Disordered Cl atoms were found for one solvent molecule $CHCl_3$ at Cl(5A), Cl(5B), Cl(6A) and Cl(6B) (s.o.f. 0.5) (Table 3). Atomic scattering factors for neutral atoms and real and imaginary dispersion terms were taken from *International Tables for X–ray Crystallography* [64]. Figs. 2 and 3 were created by SHELXTL-Plus [65]. Crystallographic data are given in Table 2, selected bond distances and angles in Table 3.

The $^{119}$Sn Mössbauer spectra (Tables 4 and 6) were obtained by the instrumentation and procedure previously reported [66,67]. Infrared spectra (KBr pellets) (Table 7) were determined on a Bruker FTIR spectrometer IFS 113V; NMR spectra (Tables 8–10) were measured on a Bruker AM 300 spectrometer ($T = 37°C$). The UV–vis absorption spectra were obtained with a Perkin–Elmer Lambda 15 instrument.

## 3. Results and discussion

The results of the elemental analyses reported in Table 1 indicate for all complexes here investigated the stoichiometry to correspond to the formula $RSnL_3$. Molecular weights in $CHCl_3$ indicate the occurrence of monomeric species (Numbers **1**–**5**, **11**, Table 1).

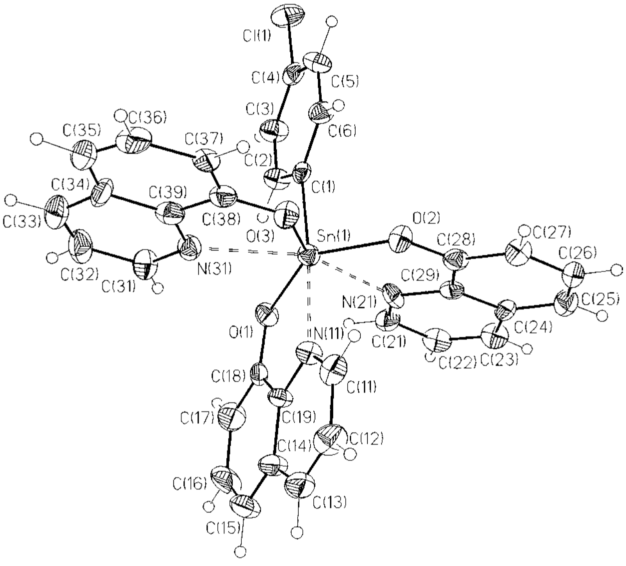

Fig. 2. General view (SHELXTL-Plus) of a molecular unit of *p*-ClPh-$Sn(Ox)_3$ (**9a**) showing 50% probability displacement ellipsoids and the atom numbering.

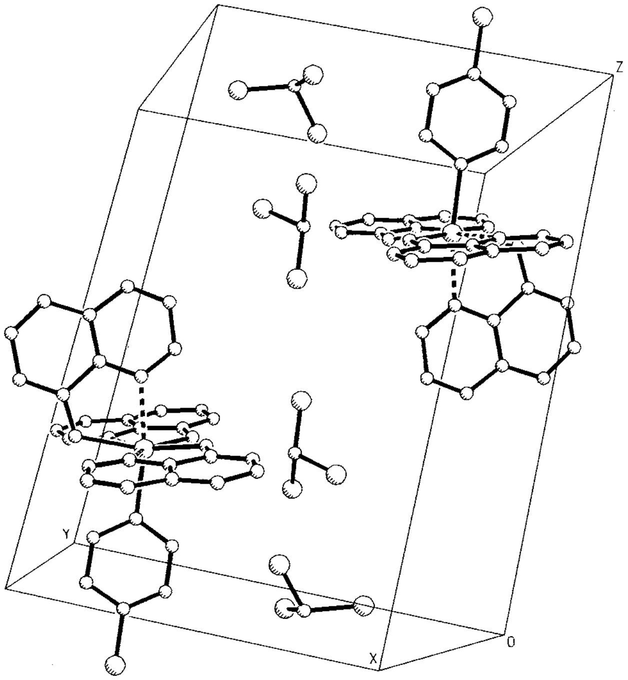

Fig. 3. View (SHELXTL-Plus) of *p*-ClPhSn(Ox)$_3$ (**9a**) showing the unit cell with four CHCl$_3$ molecules.

Comments on the syntheses of the complexes RSn(O$_2$CPy)$_3$·2H$_2$O, listed in Table 1, correspond to reports for species RSnL$_3$ (L = SPy, SPym [1]); a peculiarity of the $^-$O$_2$CPy derivatives is their content of H$_2$O molecules (as detected, inter alia, by differential thermal analysis); also the failure to separate BzHg(O$_2$CPy) from BzSn(O$_2$CPy)$_3$ is remarkable (see Section 2, this work).

The compounds RSn(Ox)$_3$, **6**–**10** in Table 1, were obtained by the reaction:

$$\mathrm{RSnCl_3 + 4\ HOx \xrightarrow{NH_3/MeOH} RSn(Ox)_3 + NH_4(Ox) + 3\ NH_4Cl} \quad (1)$$

[See Section 2.2.1, method (a)]; complex **11** (Table 1) could not be obtained by Eq. (1), but metathesis according to Eq. (2) was successful:

$$\mathrm{3\ NaOx} + o\text{-}\mathrm{ClBzSnCl_3} \rightarrow o\text{-}\mathrm{ClBzSn(Ox)_3 + 3\ NaCl} \quad (2)$$

[Section 2.2.1, method (b)]. Attempts to separate NaCl from the dried reaction mixture with H$_2$O yielded a hydrolyzed product; however, the separation of *o*-ClBzSn(Ox)$_3$ from NaCl could be effected by dissolving the oxinate complex with CHCl$_3$. This procedure could not be employed for other RSn(Ox)$_3$ species due to their insufficient solubility in CHCl$_3$. Crystals which include one mole CHCl$_3$ per mole of complex (**11**, Table 1), were obtained at −30°C after addition of petroleum ether (b.p. 30–60°C) to a concentrated solution in CHCl$_3$; single crystals *p*-ClPhSn(Ox)$_3$·2CHCl$_3$ (**9a**) separated from a saturated solution of **9** in CHCl$_3$ on standing at 4°C; the latter were submitted to X-ray diffractometry (Tables 2 and 3); CHCl$_3$ could not be removed from complex **11** even at 50°C under vacuum.

## *3.1. Structures in the solid state*

### *3.1.1. X-ray diffractometry*

No X-ray structure of species RSn(Ox)$_3$ has so far been reported in the literature. X-ray diffractometry of single crystals of *p*-ClPhSn(Ox)$_3$·2CHCl$_3$, **9a**, Tables 2 and 3 and Figs. 2 and 3, showed the complex **9a** to be monomeric, Fig. 2; four CHCl$_3$ molecules are present in the unit cell, Fig. 3, two Cl atoms in two CHCl$_3$ molecules being disordered (Table 3). The Ox ligands are bidentate, coordinating Sn through N, O atoms; two N and three O atoms yield a pentagonal plane centered on Sn, two Ox ligands lying in the equatorial plane, while the third Ox is perpendicular to the plane, with axial N and equatorial O in the axially distorted pentagonal bipyramid (Fig. 2 and Table 3).

Table 2
Crystallographic data for *p*-ClPhSn(Ox)$_3$·2CHCl$_3$ (**9a**)

| Formula | C$_{33}$H$_{22}$N$_3$O$_3$ClSn·2CHCl$_3$ (**9a**) |
|---|---|
| Formula weight | 901.41 |
| Crystal system | Triclinic |
| Crystal size, mm | 0.40 × 0.34 × 0.32 |
| Space group | $P\bar{1}$ |
| $a$ (Å) | 9.484(3) |
| $b$ (Å) | 11.968(3) |
| $c$ (Å) | 17.164(7) |
| $\alpha$ (°) | 88.94(3) |
| $\beta$ (°) | 88.46(3) |
| $\gamma$ (°) | 66.75(2) |
| $V$ (Å$^3$) | 1789.3(9) |
| $Z$ | 2 |
| $\rho_{\mathrm{calcd}}$ (Mg m$^{-3}$) | 1.673 |
| $\mu$ (mm$^{-1}$) | 1.278 |
| $F$(000) | 896 |
| Absorp. corr., type | Empirical, Ψ scan |
| $T_{\mathrm{max.}}/T_{\mathrm{min.}}$ | 0.954/0.871 |
| $\theta$ range, (°) | 1.85 to 25.05 |
| Index ranges | $-11 \leq h \leq 2$<br>$-14 \leq k \leq 13$<br>$-20 \leq l \leq 19$ |
| Reflect. Collect. | 5690 |
| Indep. Reflect./$R_{\mathrm{int}}$ | 5460/0.0250 |
| Ref. Parameters | 462 |
| Reflect. Obs. with ($I > 2\sigma(I)$) | 4675 |
| GooF (F$^2$) | 1.025 |
| $R_1$ ($F$) ($I > 2\sigma(I)$) | |
| $wR_2$ ($F^2$) (all Data) | 0.0435 (F) |
| 0.1143 (F$^2$) | |
| $(\Delta/\sigma)_{\mathrm{max.}}$ | 0.001 |
| Largest diff. peak/hole (e Å$^{-3}$) | 1.071/−0.979 |

Table 3
Selected bond distances (Å) and bond angles (°) in $p$-ClPhSn(Ox)$_3$·2CHCl$_3$ (**9a**)

*Bond distances*

| | | | | | |
|---|---|---|---|---|---|
| Sn(1)–C(1) | 2.136(4) | Sn(1)–N(21) | 2.491(4) | C(2)–C(3) | 1.386(7) |
| Sn(1)–O(1) | 2.120(3) | Sn(1)–N(31) | 2.472(4) | C(3)–C(4) | 1.395(7) |
| Sn(1)–O(2) | 2.099(3) | Cl(1)–C(4) | 1.743(5) | C(4)–C(5) | 1.367(7) |
| Sn(1)–O(3) | 2.114(3) | C(1)–C(6) | 1.395(6) | C(5)–C(6) | 1.408(7) |
| Sn(1)–N(11) | 2.205(4) | C(1)–C(2) | 1.396(6) | | |
| O(1)–C(18) | 1.308(5) | O(2)–C(28) | 1.338(6) | O(3)–C(38) | 1.335(6) |
| N(11)–C(11) | 1.311(6) | N(21)–C(21) | 1.295(6) | N(31)–C(31) | 1.331(6) |
| N(11)–C(19) | 1.354(6) | N(21)–C(29) | 1.363(6) | N(31)–C(39) | 1.354(6) |
| C(11)–C(12) | 1.425(7) | C(21)–C(22) | 1.397(7) | C(31)–C(32) | 1.403(7) |
| C(12)–C(13) | 1.368(8) | C(22)–C(23) | 1.360(7) | C(32)–C(33) | 1.345(8) |
| C(13)–C(14) | 1.415(8) | C(23)–C(24) | 1.409(7) | C(33)–C(34) | 1.414(7) |
| C(14)–C(15) | 1.415(8) | C(24)–C(25) | 1.419(7) | C(34)–C(35) | 1.406(8) |
| C(14)–C(19) | 1.423(6) | C(24)–C(29) | 1.422(6) | C(34)–C(39) | 1.422(7) |
| C(15)–C(16) | 1.357(9) | C(25)–C(26) | 1.388(7) | C(35)–C(36) | 1.366(8) |
| C(16)–C(17) | 1.405(8) | C(26)–C(27) | 1.398(7) | C(36)–C(37) | 1.430(7) |
| C(17)–C(18) | 1.385(7) | C(27)–C(28) | 1.390(6) | C(37)–C(38) | 1.352(7) |
| C(18)–C(19) | 1.464(7) | C(28)–C(29) | 1.425(6) | C(38)–C(39) | 1.432(7) |
| C(41)–Cl(2) | 1.757(6) | C(51)–Cl(5A) [a] | 1.749(9) | C(51)–Cl(6B) [a] | 1.85(2) |
| C(41)–Cl(3) | 1.781(7) | C(51)–Cl(6A) [a] | 1.652(13) | C(51)–Cl(7) | 1.747(6) |
| C(41)–Cl(4) | 1.759(6) | C(51)–Cl(5B) [a] | 1.804(9) | | |

*Bond angles*

| | | | |
|---|---|---|---|
| O(2)–Sn(1)–O(3) | 74.14(12) | C(5)–C(4)–Cl(1) | 119.4(4) |
| O(2)–Sn(1)–O(1) | 139.76(12) | C(3)–C(4)–Cl(1) | 118.7(4) |
| O(3)–Sn(1)–O(1) | 138.69(12) | C(18)–O(1)–Sn(1) | 117.6(3) |
| O(2)–Sn(1)–C(1) | 100.73(14) | C(11)–N(11)–Sn(1) | 126.0(3) |
| O(3)–Sn(1)–C(1) | 100.57(14) | C(19)–N(11)–Sn(1) | 113.2(3) |
| O(1)–Sn(1)–C(1) | 94.97(14) | C(28)–O(2)–Sn(1) | 123.3(3) |
| O(2)–Sn(1)–N(11) | 86.51(13) | C(21)–N(21)–Sn(1) | 129.9(3) |
| O(3)–Sn(1)–N(11) | 86.85(13) | C(29)–N(21)–Sn(1) | 110.8(3) |
| O(1)–Sn(1)–N(11) | 75.80(13) | C(38)–O(3)–Sn(1) | 122.5(3) |
| C(1)–Sn(1)–N(11) | 170.77(14) | C(31)–N(31)–Sn(1) | 129.7(3) |
| O(2)–Sn(1)–N(31) | 144.76(13) | C(39)–N(31)–Sn(1) | 111.0(3) |
| O(3)–Sn(1)–N(31) | 70.63(13) | Cl(2)–C(41)–Cl(4) | 110.4(4) |
| O(1)–Sn(1)–N(31) | 72.42(13) | Cl(2)–C(41)–Cl(3) | 108.2(3) |
| C(1)–Sn(1)–N(31) | 86.53(14) | Cl(4)–C(41)–Cl(3) | 109.4(3) |
| N(11)–Sn(1)–N(31) | 90.83(14) | Cl(6A) [a]–C(51)–Cl(7) | 112.9(6) |
| O(2)–Sn(1)–N(21) | 70.65(12) | Cl(6A) [a]–C(51)–Cl(5A) [a] | 82.8(7) |
| O(3)–Sn(1)–N(21) | 144.43(12) | Cl(7)–C(51)–Cl(5A) [a] | 110.9(4) |
| O(1)–Sn(1)–N(21) | 72.33(12) | Cl(6A) [a]–C(51)–Cl(5B) [a] | 117.9(7) |
| C(1)–Sn(1)–N(21) | 90.79(14) | Cl(7)–C(51)–Cl(5B) [a] | 106.0(4) |
| N(11)–Sn(1)–N(21) | 86.19(13) | Cl(7)–C(51)–Cl(6B) [a] | 103.9(6) |
| N(31)–Sn(1)–N(21) | 144.26(12) | Cl(5A) [a]–C(51)–Cl(6B) [a] | 99.4(6) |
| C(6)–C(1)–Sn(1) | 121.5(3) | Cl(5B) [a]–C(51)–Cl(6B) [a] | 134.7(6) |
| C(2)–C(1)–Sn(1) | 119.6(3) | | |

[a] Site occupancy factor 0.5.

### 3.1.2. $^{119}$Sn Mössbauer spectroscopy: structure and dynamics

High quality $^{119}$Sn Mössbauer spectra, measured for the complexes listed in Table 4, were obtained, as shown in Fig. 4. The latter is quite surprising and unexpected for BzSn(O$_2$CPy)$_3$, considering the failure to separate a pure compound (see Section 2.2). In fact, the sample submitted to Mössbauer spectroscopy (Table 4) showed the following analytical data, found (Anal. Calc.)%: C, 45.12 (49.05); H, 2.85 (3.79); N, 5.27 (6.86); the parameters in Table 4 clearly indicate that the species BzSn(O$_2$CPy)$_3$, as part of the reaction mixture obtained, is a complex with a fully regular structure, corresponding to that of the other derivatives in the Table.

The Mössbauer parameters listed in Table 4 are typical for mono-organotin derivatives [68]. In particular, data insert quite well into $\delta$ and $\Delta E$ values reported for aryltin(IV) derivatives characterized by three tin–oxygen bonds [69]. Substantial differences are detected with respect to ArSn(S,N)$_3$ complexes [1], where larger isomer shift values occur, owing to S → Sn charge transfer [1]; besides, a wider interval for nuclear quadrupole splitting data has been interpreted to be due to the occurrence of a series of structures [1].

On the contrary, the parameters inherent to the

Table 4
$^{119}$Sn Mössbauer parameters of mono-organotin(IV) complexes with pyridine-2-carboxylic acid and 8-hydroxyquinoline

| Number | Compound [a] | $\delta$ [b,c] (mm $s^{-1}$) | $\Delta E$ [b,d] (mm $s^{-1}$) | $\Gamma_1$; $\Gamma_2$ [b,e] (mm $s^{-1}$) |
|---|---|---|---|---|
| **1** | $p$-TolSn$(O_2CPy)_3 \cdot 2H_2O$ | 0.61 | 1.82 | 0.81 |
| **2** | $o$-TolSn$(O_2CPy)_3 \cdot 2H_2O$ | 0.62 (0.611 ± 0.003) | 1.87 (1.842 ± 0.009) | 0.85 (0.819 ± 0.008) |
| **3** | $p$-ClPhSn$(O_2CPy)_3 \cdot 2H_2O$ | 0.61 (0.609 ± 0.004) | 1.82 (1.840 ± 0.012) | 0.90 (0.890 ± 0.027) |
| **4** | $o$-ClPhSn$(O_2CPy)_3 \cdot 2H_2O$ | 0.55 | 1.62 | 0.92 |
| **5** | $o$-ClBzSn$(O_2CPy)_3 \cdot 2H_2O$ | 0.69 (0.686 ± 0.003) | 1.82 (1.816 ± 0.004) | 0.84 (0.846 ± 0.009) |
| **5′** | BzSn$(O_2CPy)_3$ [f] | 0.74 | 1.83 | 0.84 |
| **6** | PhSn$(Ox)_3$ | 0.59 (0.584 ± 0.005) | 2.02 (2.015 ± 0.004) | 0.80 (0.783 ± 0.011) |
| **7** | $p$-TolSn$(Ox)_3$ | 0.60 | 1.82 | 0.86 |
| **8** | $o$-TolSn$(Ox)_3$ | 0.60 (0.593 ± 0.007) | 1.68 (1.681 ± 0.009) | 0.79 (0.794 ± 0.016) |
| **9** | $p$-ClPhSn$(Ox)_3$ | 0.56 | 1.71 | 0.82 |
| **10** | $o$-ClPhSn$(Ox)_3$ | 0.52 (0.511 ± 0.012) | 1.57 (1.558 ± 0.008) | 0.86 (0.844 ± 0.011) |
| **11** | $o$-ClBzSn$(Ox)_3 \cdot CHCl_3$ | 0.63 | 1.57 | 0.90 |

[a] See Table 1 for abbreviations.

[b] Determined at 77.3 K on finely powdered solid absorber samples. Data in parentheses: average values in the $T$ ranges reported in Table 6, with standard error.

[c] Isomer shift with respect to r.t. $Ca^{119}SnO_3$.

[d] Nuclear quadrupole splitting.

[e] Full width at half height. The spectra were fitted as symmetrical doublets with NORMOS program.

[f] Mixture with the solid complex of BzHg$^{II}$, see Sections 2 and 2.2.

$^-O_2CPy$ and $Ox^-$ complexes here investigated (Table 4) are generally corresponding; besides, in some instances $\delta$ and $\Delta E$ for couples of derivatives with a given Ar are almost identical (Table 4). One is then tempted to conclude that the same structure of tin environments occurs for all complexes listed in Table 4.

For proving this assumption, the starting point could be the crystal and molecular structure of $p$-ClPhSnOx$_3$, Tables 2 and 3 and Figs. 2 and 3, which is the only one reported in the literature for $RSn(L)_3$ complexes, L = $^-O_2CPy$ and $Ox^-$; this structure type is also sketched in Table 5 (I), bond angles being idealized according to a regular structure. The same could be assumed for all $RSn(Ox)_3$ derivatives here investigated: in fact, X-ray diffractometry of a series of complexes $R_2Sn(Ox)_2$ 2,15,16,19b, $R_2SnClOx$ [17] and $RSnCl(Ox)_2$ [18] all show the occurrence of N, O chelation of tin by the ligand. In the case of $^-O_2CPy$ complexes of organotin(IV) acceptors, single crystal X-ray diffractometry reveals a series of possible coordination situations, from $Me_2SnCl(O_2CPy)$ where the ligand behaves as tridentate through N, O, O yielding a polymeric species with 6-coordinated tin [3], to $Me_2Sn(O_2CPy)_2$ with 7-coordinated tin, into a polymeric species, due to one bridging (tridentate) ligand [4], to $Me_3Sn(O_2CPy) \cdot H_2O$ [7], and $Ph_3SnCl(O_2CPy(H))$ [8] with monodentate –COO$^-$ and trigonal bipyramidal tin environment; $^-O_2CPy$ then acts as mono-, bi- and tridentate. Anyhow, the maximum tin coordination number detected is seven.

On these grounds, structural assignments by the point-charge model formalism [70–72] through calculation of $\Delta E$ parameters have been attempted for the complexes in Table 4. Partial nuclear quadrupole splittings, pqs, inherent to five-coordinated tin structures [71,72] were applied to pentagonal bipyramidal configurations [73,74]. Anyhow, no pqs data for (Ox)O$^-$ and (Py)COO$^-$ in trigonal bipyramidal structures, to be

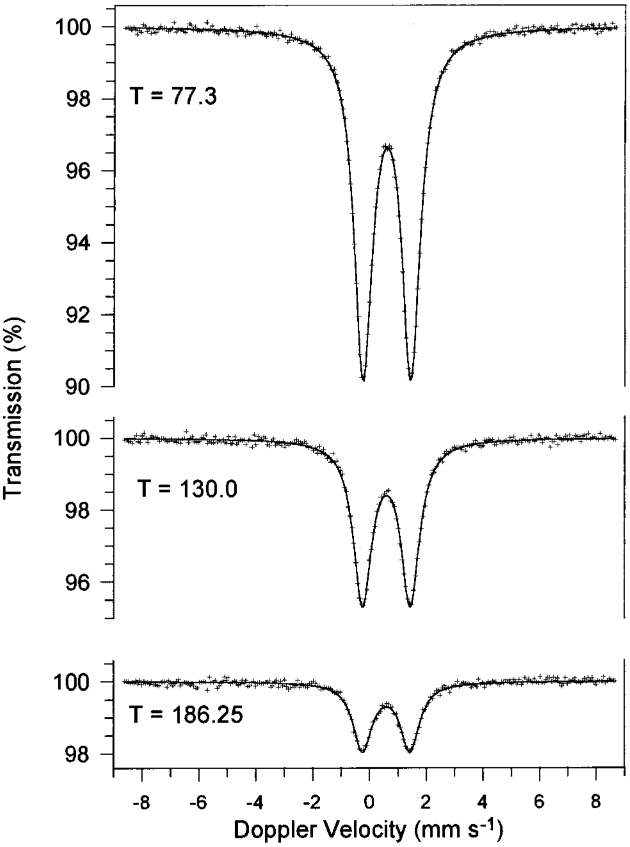

Fig. 4. The quality of variable temperature $^{119}$Sn Mössbauer spectra measured in the present study: data for $o$-TolylSn$(Ox)_3$ (Number **8**, Tables 4 and 6).

Table 5

Point-charge model (Refs. [70–72]) estimates of the partial nuclear quadrupole splitting, pqs, $\{(Ox)O\}^{pbe}$, inherent to the oxygen atom of 8-hydroxyquinoline bound to Sn in pentagonal bipyramidal $RSn(Ox)_3$ complexes (equatorial position), and the determination of its reliability from calculations of the nuclear quadrupole splittings, $\Delta E$, for $RSn(Ox)_3$ and $R_3Sn(Ox)$ complexes [a]

| Number | Compound | $\Delta E_{exp}$ (mm $s^{-1}$) | Refs. | Structure | $\{(Ox)O\}^{pbe}$ (mm $s^{-1}$) |
|---|---|---|---|---|---|
| (A) Calculations of $\{(Ox)O\}^{pbe}$ | | | | | |
| 1. | $p$-ClPhSn(Ox)$_3$ | 1.71 | This work (Table 4) | (I) | $-0.312$ [b] |
| 2. | $^n$BuSn(Ox)$_3$ | (+)1.82 [c] ($\eta = 0.2$) [d] | 28 | (I) | $-0.182$ |
| (B) | Calculations of $\Delta E$ [e] | | | | |
| | Compound or class of compounds | $\Delta E_{exp}$ or range (mms$^{-1}$) | Refs. | Structure | $\Delta E_{calcd}$ (mms$^{-1}$) |
| 3. | ArylSn(Ox)$_3$ | 1.57–2.02 | This work (Table 4) | (I) | (+)1.84; $\eta$ [d] = 0.99 |
| 4. | AlkylSn(Ox)$_3$ [f] | 1.67–2.18 | 21, 25, 28, 30 | (I) | (+)1.93; $\eta$ [d] = 0.94 |
| 5. | Ph$_3$Sn(Ox) [g] | (−)1.75 [c] ($\eta = 0.7$) [d] | 28 | (II) | |
| 6. | Ph$_3$Sn(Ox) [g] | 1.69−2.36 | 6, 21, 30, 32 | (II) | (−)2.02; $\eta$ [d] = 0.46 |
| 7. | Ph$_3$Sn(Ox) [h] | 1.53 [i]; 2.57 [i] | 30 | (II) | |
| 8. | Me$_3$Sn(Ox) | 2.27 | 6 | (II) | (−)2.24; $\eta$ [d] = 0.68 |

[a] Abbreviations: Me = methyl; Et = ethyl; Bu = butyl; Ph = phenyl; Bz = benzyl; HOx = 8–hydroxyquinoline and derivatives (see notes). Partial nuclear quadrupole splitting values, mms$^{-1}$, employed in the calculations (Refs. [71,74]): $\{Alk\}^{tba} = -0.94$; $\{Alk\}^{tbe} = -1.13$; $\{Aryl\}^{tba} = \{Bz\}^{tba} = -0.89$; $\{Aryl\}^{tbe} = -0.98$; $\{N_{het}\}^{tba} = -0.035$; $\{N_{het}\}^{tbe} = +0.147$; see also footnote (e). tba = trigonal bipyramidal axial, tbe = trigonal bipyramidal equatorial. These values are assumed to hold also for pentagonal bipyramidal structures (see Ref. [73]; equatorial, pbe; axial, pba).

[b] $\Delta E_{calcd}$ with this pqs value shows a negative sign. The employment of the crystallographic angles (Table 3) does not consistently vary the calculated parameters.

[c] Sign of $\Delta E$ obtained from the Mössbauer–Zeeman spectrum (Ref. [28]).

[d] Asymmetry parameter $\eta = V_{xx} - V_{yy}/V_{zz}$ (Refs. [70–72]).

[e] Employing the values $\{(Ox)O\}^{pbe} = -0.182$ mm s$^{-1}$, and $\{(Ox)O\}^{pba,tba} = -0.282$ mm s$^{-1}$; the latter is obtained from $\{(Ox)O\}^{pbe} = -0.182$ mm s$^{-1}$, assumed to hold also for trigonal bipyramidal structures, employing the relationship $[3\{L\}^{the} - 4\{L\}^{tba}] = 0.58$ mm s$^{-1}$ (Ref. [71]). Other pqs values: see footnote (a).

[f] Alkyl = Bu, HOx = 8-hydroxyquinoline; Alkyl = Et, HOx = (5,7-dichloro)-; (5,7-dibromo)-; (5-nitro)-; -8-hydroxyquinoline.

[g] HOx = 8-hydroxyquinoline [6,21]; = (5,7-dichloro)–; (5,7-dibromo)–; (5-COCH$_3$)–; (5-COC$_6$H$_5$)–; (5-N=N–C$_6$H$_5$)–; -8-hydroxyquinoline [30,32].

[h] HOx = (2-CH$_3$)–; (5,7-diiodo)–; -8-hydroxyquinoline.

[i] Out of correlation $|\Delta E_{exp} - \Delta E_{calcd}| = 0.4$ mms$^{-1}$: M.G. Clark, A.G. Maddock, R.H. Platt, J. Chem. Soc. Dalton Trans. (1972) 281. In structures (I) and (II), $x, y, z$ are the principal axes of the electric field gradient tensor (Refs [70–72]).

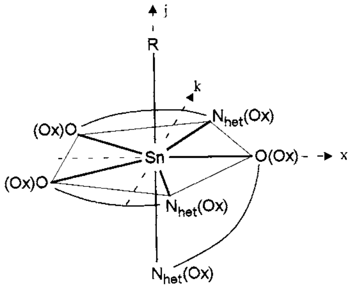

Structure (I)

Regular pentagonal bipyramidal structure (idealized, from the X-ray structure of $p$-ClPhSn(Ox)$_3$, Figs. 2 and 3).
Compound **1**: j = y, k = z: (-)$\Delta E_{calcd}$
Compounds **2-4**: j = z, k = y: (+)$\Delta E_{calcd}$

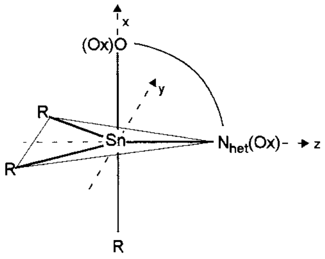

Structure (II)

Regular (idealized) trigonal bipyramidal structure (Refs. [28, 30, 32]).

employed in complexes of Ar$Sn^{IV}$ with 8-hydroxyquinoline and pyridine-2-carboxylic acid, respectively, have been insofar reported: for 8-hydroxyquinoline, data related to Ox/2 are quoted [71,72], and existing values for –COO$^-$ concern carboxylate groups from aliphatic acids [71,72] and amino acids [75], which cannot be reliably employed in the present context. We then proceed to argue as follows: (i) we assume an idealized regular pentagonal bipyramidal structure for $p$-ClPhSnOx$_3$, (I) in Table 5, corresponding to the determined crystal and molecular structure, Figs. 2 and 3; (ii) employing the experimental value $\Delta E = 1.71$ mms$^{-1}$, Table 4, as well as the pqs values listed in Table 5, the pqs $\{(Ox)O\}^{pbe}$ is calculated (Table 5, [68,70–73]); (iii) the value thus obtained is adjusted in order to yield a positive sign for $\Delta E_{calcd}$, according to the Mössbauer–Zeeman spectrum of $^n$BuSnOx$_3$ (Table 5) [28]; (iv) the reliability of the latter pqs value is checked by point-charge model estimates of $\Delta E$ for pentagonal bipyramidal $RSnOx_3$ and trigonal bipyramidal $R_3SnOx$ complexes whose $\Delta E$ data are quoted in the literature (Table 5).

From the data in Table 5, it is concluded that the pqs values $\{(Ox)O^-\}^{pbe} = -0.182$ mm $s^{-1}$, and the related $\{(Ox)O^-\}^{pba,tba} = -0.282$ mm $s^{-1}$, are highly reliable, and that all $ArSnOx_3$ complexes in Table 4 show the same structure, of type (I) in Table 5. As far as the $ArSn(O_2CPy)_3$ complexes are concerned, for which no crystal and molecular structures are available, we are inclined to assume that the pqs for $\{(Py)COO^-\}^{pbe}$ corresponds to the value for $\{(Ox)O^-\}^{pbe}$, the structure being then corresponding to that for $ArSnOx_3$ in Figs. 2 and 3, and in Table 5, with seven coordinated Sn. In fact, $H_2O$ molecules in the $^-O_2CPy$ complexes (Table 1) could be hydrogen bonded to carboxyl oxygens although possibly bound to the metal [7]. Further work is obviously needed on the latter argument.

Structural information may be extracted also from variable temperature $^{119}$Sn Mössbauer spectroscopy data and functions. From the data $\delta$, $\Delta E$ and $\Gamma$ in Table 4, measured in the $T$ ranges reported in Table 6, inherent to the representative complexes **2**, **3**, **5**, **6**, **8**, **10**, the following is inferred:

1. The invariability of $\delta$ and $\Delta E$ parameters indicate the lack of phase transitions [76], as well as of $\delta$'s second-order Doppler shifts [77];
2. The areas under the two resonant peaks, e.g. Fig. 4, are symmetric, which excludes anisotropy for the recoil-free fractions $f_a$ [78];
3. The narrowness of $\Gamma$ indicates the persistence of single tin coordination sites in the related $T$ ranges. Molecular dynamics data and functions (as e.g. defined and treated in a recent review [68]) in Table 6 and Figs. 5 and 6, suggest the following:
4. The linearity of functions $\ln A(T)$, $f_a^{rel,abs}(T)$ and $\langle x^2\rangle(T)$ further implies the general absence of phase transitions;
5. Parameters and functions extracted from slopes $d\ln A/dT$ ('relative') [68] and from the recoil free fraction of the source ('absolute') [68] are practically coincident, which implies the nature of Debye solids [68] for the complexes here investigated;
6. Parameters and functions for the complexes **2**, **3**, **5**, **6**, **8**, **10** are mutually corresponding, which suggests the occurrence of strict structural analogies. In particular, by fingerprint criteria [68], $\vartheta_D$ values are typical for monomeric species, while slopes $d\ln A/dT$, functions $\langle x^2\rangle(T)$ and parameters $M\vartheta_D^2$ lie in monomer polymer border zones [68].

It is concluded that the complexes listed in Table 6 show structures which imply the lack of intermolecular interactions (including H-bonds by $H_2O$ molecules, and bridging by –COO groups, in $RSn(O_2CPy)\cdot 2H_2O$ complexes), possibly corresponding to the structure determined for $p$-ClPhSn$(Ox)_3$, Fig. 2, and assumed for $RSn(Ox)_3$ in Table 5. The nature of the R radicals in $RSn(L)_3$, as well as the occurrence of $o$- and $p$- substituent in R, would then show no structural influence in the complexes. It would then be inferred that all species in Table 1 show analogous structures, possibly of pentagonal bipyramidal type.

It seems worth to note that complexes $RSn(SPy)_3$, where $SPy^-$ is the bidentate N, S ligand anion from 2-mercaptopyridine, belong to the class of $RSn(Ox)_3$ and $RSn(O_2CPy)_3$ species, three members of the series (R = Me, Ph, $p$-Tolyl) showing a pentagonal bipyramidal X-ray structure [1,79], and exhibit dynamical data [74,80] quite similar to those for $Ox^-$ and $^-O_2CPy$ complexes reported here (Table 6). These circumstances further support the assumption of 'monomeric' structures for all members of the class of $RSnL_3$ species commented above.

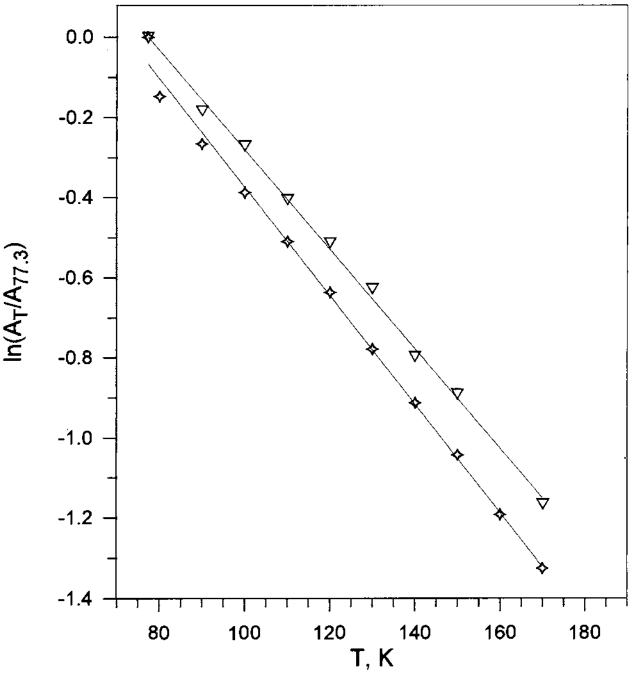

Fig. 5. Examples for the temperature dependence of the normalized total Lorentzian areas, A, under the $^{119}$Sn Mössbauer peaks. ◇ $PhSnOx_3$ (**6**), ▽ $o$-Cl-BzSn$(O_2CPy)_3$ (**5**). Lines are the least squares fits of the linear functions to the experimental data points, the related equations being: ◇ $\ln(A_T/A_{77.3}) = 0.980-1.355\times 10^{-2}$ T; ▽ $\ln(A_T/A_{77.3}) = 0.961-1.242\cdot 10^{-2}$ T.

Table 6
Variable temperature $^{119}$Sn Mössbauer spectroscopy measurements: experimental data sets, and molecular dynamics data functions

| Number | Compound [a] | $T_{max}$ in the $T$ range investigated $77.3 \div T_{max}$ (K) | $10^2(\mathrm{d}\ln A/\mathrm{d}T)$ [b] ($K^{-1}$) | $f_a(T)$ [c,d] | $\langle x^2\rangle(T)$ [d] ($Å^2 \times 10^2$) | $\vartheta_D$ [e,f,h] (K) | $\tilde{\nu}_D$ [f,h] ($cm^{-1}$) | $M\vartheta_D^2$ [g,h] (amu × $K^2 \times 10^{-6}$) |
|---|---|---|---|---|---|---|---|---|
| **2** | $o$-TolSn($O_2$CPy)$_3$·2$H_2O$ | 170.0 | −1.397 (0.999) | 0.340 ÷ 0.093<br>(0.489 ÷ 0.121) | 0.739 ÷ 1.626<br>(0.490 ÷ 1.445) | 49.9 (55.7 ± 2.5) | 34.7 (38.7 ± 1.7) | 1.524 |
| **3** | $p$-ClPhSn($O_2$CPy)$_3$·2$H_2O$ | 180.0 | −1.392 (0.994) | 0.341 ÷ 0.082<br>(0.462 ÷ 0.091) | 0.737 ÷ 1.716<br>(0.528 ÷ 1.642) | 49.2 (52.1 ± 2.7) | 34.2 (36.2 ± 1.9) | 1.531 |
| **5** | $o$-ClBzSn($O_2$CPy)$_3$·2$H_2O$ | 170.0 | −1.242 (0.999) | 0.383 ÷ 0.121<br>(0.467 ÷ 0.137) | 0.658 ÷ 1.446<br>(0.521 ÷ 1.362) | 52.8 (55.2 ± 1.1) | 36.7 (38.3 ± 0.8) | 1.714 |
| **6** | PhSn(Ox)$_3$ | 170.0 | −1.355 (0.998) | 0.351 ÷ 0.100<br>(0.413 ÷ 0.103) | 0.717 ÷ 1.577<br>(0.605 ÷ 1.557) | 50.0 (51.1 ± 1.1) | 34.7 (35.5 ± 0.8) | 1.571 |
| **8** | $o$-TolSn(Ox)$_3$ | 186.25 | −1.421 (0.999) | 0.333 ÷ 0.071<br>(0.372 ÷ 0.071) | 0.752 ÷ 1.812<br>(0.678 ÷ 1.809) | 48.3 (49.2 ± 0.8) | 33.5 (34.2 ± 0.5) | 1.498 |
| **10** | $o$-ClPhSn(Ox)$_3$ | 170.0 | −1.461 (0.999) | 0.323 ÷ 0.083<br>(0.383 ÷ 0.089) | 0.773 ÷ 1.701<br>(0.657 ÷ 1.658) | 46.9 (48.5 ± 1.0) | 36.2 (33.7 ± 0.7) | 1.458 |

[a] Abbreviations: see Fig. 1 and note (a) to Table 1. The molecular weights (including 2$H_2O$ for compounds **2**, **3**, **5**) have been employed as the effective vibrating mass, EVM, in the calculations.

[b] $A = (\pi/2)\varepsilon\Gamma$, mm $s^{-1}$, is the total Lorentzian area under the resonant peaks at the temperature $T$ (K). $\varepsilon$ = percent resonant effect; $\Gamma$ = full width at half height of the resonant peaks. Slopes of functions: total area under the resonant peaks versus temperature (see Fig. 4).

[c] The recoil-free fraction (Debye–Waller–Mössbauer factor).

[d] The mean square displacement of $^{119}$Sn atoms. Values in the first line are 'relative' data obtained from slopes $\mathrm{d}\ln A/\mathrm{d}T$, at 77.3 K and $T_{max}$, respectively; values in parentheses are the 'absolute' data at 77.3 K and $T_{max}$.

[e] Debye temperature.

[f] Debye cut-off frequency. First line, 'relative' data; values in parentheses, 'absolute' data, with standard error, calculated from $f_a^{abs}$.

[g] Parameter of intermolecular force constant, calculated for $M$ = molecular mass (including 2$H_2O$ for Numbers **2**, **3**, **5**) and $\vartheta_D$ = 'relative' Debye temperature.

[h] For complexes **2**, **3** and **5**, data essentially corresponding to the tabulated values have been obtained by employing EVM = MW without 2$H_2O$.

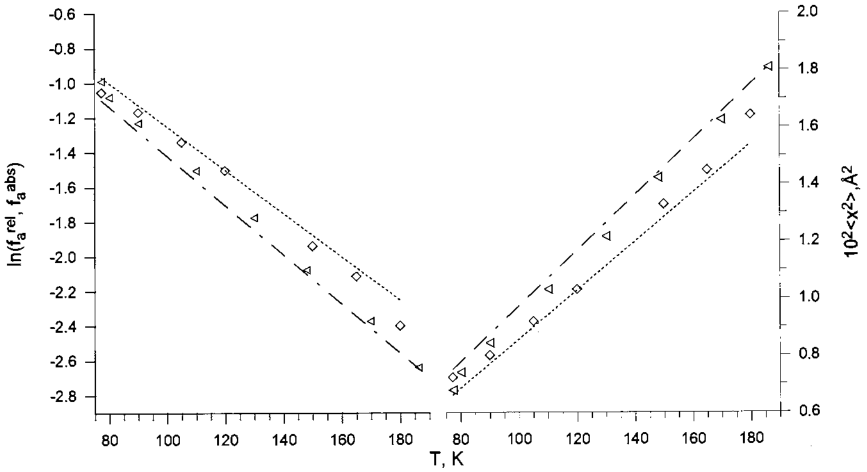

Fig. 6. Recoil-free fractions of the absorber $^{119}$Sn nuclei, $f_a$, and mean-square displacements of $^{119}$Sn, $\langle x^2 \rangle$, as a function of temperature, for representative $RSnL_3$ complexes. Lines are plots of $f_a^{rel}$, and the related $\langle x^2 \rangle$ functions, as extracted from the slopes d ln $A_t$/d$T$, while data points are 'absolute' data, $f_a^{abs}$, and corresponding $\langle x^2 \rangle$. *o*-TolylSn(Ox)$_3$ (**8**), ◁ and – – –; *p*-ClPhSn($O_2CPy$)$_3$ (**3**), ◇ and · · · ·.

### *3.1.3. Vibrational spectroscopy*

The structural assumptions reported in the preceding were checked by studying the vibrational data reported in Table 7. In compounds **1**–**5**, $RSn(O_2CPy)_3 \cdot 2H_2O$, the carboxylate group would coordinate Sn in a monodentate fashion; in fact, $\nu_{as}$(OCO) around 1680 cm$^{-1}$ suggest the occurrence of free C=O, while $\nu_s$(OCO) in the range 1331–1408 cm$^{-1}$ is typical of a coordinated carboxyl oxygen (Table 7). These data and assumptions correspond to findings reported for a series of $Sn^{IV}$ and $R_nSn^{IV}$ ($n = 2, 3$) pyridyl carboxylate complexes. In fact, *inter alia*, the occurrence of monodentate carboxyl bound to Sn has been assumed to occur for: Snhal($O_2CPy$)$_3$ [5]; Snhal$_2$($O_2CPy$)$_2$ [5] (hal = Cl, Br); $R_2Sn(O_2CPy)_2$ [5,11]; $R_2Sn$–($O_2CPy$)$_2$, –(Py-3-$CO_2$)$_2$ and –(Py-4-$CO_2$)$_2$ [12]; $^t$Bu$_2$Sn($O_2CPy$)$_2$ [14]; $^n$Bu$_3$Sn–($O_2CPy$), –(Py-3-$CO_2$) and –(Py-4-$CO_2$) [10].

No information on the possible occurrence of N → Sn bonds in $RSn(O_2CPy)_3 \cdot 2H_2O$ can be extracted from modes $\nu_{as,s}$(C=C/N=C) listed in Table 7; in fact, inter alia, the related vibrational data of $Me_3Sb$-(Py–$CH_2$–$CO_2$)$_2$ [81] and $Me_2Sn(O_2CPy)_2$ [12], practically coincide, though these compounds are characterized by the absence [81] and the occurrence [12], respectively, of N → metal coordination. In addition the vibrational spectra of $RSn(O_2CPy)_3 \cdot 2H_2O$ contain no information on the occurrence of tin coordination by the two $H_2O$ molecules.

It is concluded that, according to the IR data, complexes $RSn(O_2CPy)_3 \cdot 2H_2O$, Table 7, Numbers **1**–**5**, consist of monomeric species, in line with the results obtained from variable temperature $^{119}$Sn Mössbauer spectroscopy studies (vide supra).

As far as complexes RSn(Ox)$_3$, Numbers **6**–**11**, are concerned, the vibrational frequencies listed in Table 7 essentially correspond to data reported in the literature for the complexes: RSn(Ox)$_3$ (R = $^n$Bu [19b,21], Et [45], Me [19b]); RSnCl(Ox)$_2$ (R = $^n$Bu [19b,21], Ph [19b,21], Me [19b,39]); $R_2$Sn(Ox)$_2$ (R = Alk [19b,21,35], $MeOCOCH_2CH_2$ [34]); $R_2$SnCl(Ox) (R = Alk [19b,21,39], $MeOCOCH_2CH_2$ [34]); $R_3$SnOx (R = Me [39], Et [45], $^t$Bu [19b], Cy [19b], Ph 19b,45) (Ox = 8-hydroxyquinoline [19b,21,34,35,39], and = halogeno- and nitro-substituted 8-hydroxyquinoline [45]). In all complexes, Ox$^-$ ligands are assumed to chelate tin through coordination by O, N atoms.

In conclusion, taking also into account the correspondence of the spectra of the complexes **6**–**11**, Table 7, the vibrational data suggest the occurrence of a general pentagonal bipyramidal structure for RSn(Ox)$_3$, analogous to that determined for *p*-ClPhSn(Ox)$_3$, Fig. 2 and Table 3.

## *3.2. Structures in solution*

### *3.2.1. $^1$H-, $^{13}$C-, $^{119}$Sn-NMR spectroscopy*

The complexes $RSn(O_2CPy)_3$ and RSn(Ox)$_3$ have been investigated in $CDCl_3$ solutions by $^1$H-, $^{13}$C- and $^{119}$Sn-NMR spectroscopy, and the results obtained are compiled in Tables 8–10.

Chemical shifts $\delta$ ($^1$H) and $\delta$ ($^{13}$C) inherent to ligand atoms in $RSn(O_2CPy)_3$ have been assigned by comparison with the spectra of the free ligand, pyridine-2-carboxylic acid [82,83] as well as of the complex $^t$Bu$_2$Sn($O_2CPy$)$_2$, where the ligand chelates Sn through –COO$^-$ (monodentate) and the N atom [14]. Shifts $\delta$ ($^1$H) and $\delta$ ($^{13}$C) related to the organic radicals bound to Sn have been assigned on the basis of the related data for $R_4Sn$ compounds [19,84]. Signal integrations indicate the stoichiometry $RSn(O_2CPy)_3$.

Complexes **1**–**5′** in Table 8 (I) generally show a broad signal for H-6 (which is the nearest one to N, Fig. 1), shifted to low field with respect to the value for ${}^{t}$Bu$_2$Sn(O$_2$CPy)$_2$ [14], which could be interpreted in terms of weak N → Sn interactions, possibly not due to all three $^-$O$_2$CPy ligands. Shifts are larger for the *o*-substituted ArSn$^{IV}$ acceptors, **2** and **4** in Table 8, with respect to the corresponding *p*-substituted species, **1** and **3**, which is attributed to the decrease in the extent of N → Sn coordination owing to steric effects due to the *o*-substituents in the organic radicals bound to tin. Analogous effects have been detected to occur in RSn(-SPy)$_3$ complexes [1].

The H atoms in the –CH$_2$– groups bound to tin in the benzyl derivatives are strongly deshielded due to tin bonding by the carboxylic group of the ligand, as shown by the magnitude of the coupling constants $^2J(^{119}\mathrm{Sn}^1\mathrm{H})$ for complexes **5** and **5′** (Table 8, footnotes e, f) with respect to data for the corresponding R$_4$Sn derivatives [19,84]; these data would be in agreement with the decrease of the s-character of the C(Bz)–Sn bonds on going from 4- to 7-coordination, the latter assumed for the RSn(O$_2$CPy)$_3$ complexes (*vide supra*).

In the $^{13}$C-NMR spectra [Table 9 (I)] parameters δ ($^{13}$C) for ligand atoms LC-2 to LC-6, as well as LC = O (Fig. 1), correspond to data reported for ${}^{t}$Bu$_2$Sn(O$_2$CPy)$_2$ [14]; moreover, broad signals occur for LC-2, LC-4 and LC-6 atoms in the complexes, due to the similarity of the respective chemical shifts, in a special way for LC-2 and LC-6 (the latter according to free ligand shifts [83]).

The broad signals δ ($^{13}$C) for LC-2 and LC-6 further suggest the occurrence of both bi- and mono-dentate $^-$O$_2$CPy species (vide supra). In the organic radicals bound to tin, nuclei C-1 and C-8 (Fig. 1(C)) are deshielded going from R$_4$Sn [19a,84] to RSn(O$_2$CPy)$_3$, clearly owing to the increase of the acid character of Sn due to coordination by the carboxylic group.

Signals δ ($^1$H) and δ ($^{13}$C) for ligand atoms in RSn(Ox)$_3$, Table 8(II) and Table 9(II), have been attributed by comparison with spectral data reported for the free ligand 8-quinolinol, HOx, as well as Ox$^-$ and H$_2$Ox$^+$ [19b,34,44,55]; besides, with data for complexes ${}^{n}$BuSn(Ox)$_3$ [19b,43]. Signals concerning H and C atoms in the organic radicals bound to Sn were attributed according to data for R$_4$Sn [19a,84]. The ratios of integrated signals generally indicate the occurrence of species with stoichiometry RSn(Ox)$_3$, Numbers **6**–**11**, in CDCl$_3$ solutions.

Chemical shifts inherent to ligand atoms H-2, H-4, LC-2 and LC-8, Table 8(II) and Table 9(II), in the complexes RSn(Ox)$_3$ here investigated are essentially in ranges reported for R$_3$Sn(Ox), R$_2$Sn(Ox)$_2$, R$_2$Sn(X)(Ox) and RSnhal(Ox)$_2$, all species being characterized by chelating Ox$^-$ [34,44,54–56]; strong N → Sn interactions shift downfield the H-2 resonance of Ox$^-$ [44]

Table 7

Infrared spectral data for mono-organotin(IV) derivatives of pyridine-2-carboxylic acid and 8-hydroxyquinoline

| Number | Compound [a] | $\nu_{as}$(OCO) (cm$^{-1}$) | $\nu_s$(OCO) (cm$^{-1}$) | Δν | $\nu_{as,s}$(C=C/N=C) (cm$^{-1}$) | |
|---|---|---|---|---|---|---|
| (I) | RSn(O$_2$CPy)$_3$·2H$_2$O | | | | | |
| **1** | *p*-TolSn(O$_2$CPy)$_3$·2H$_2$O | 1687 vs,1670 vs | 1336 vs,1408 vs | 351, 262 | 1605 s; 1560 s; 1555 s; 1478 s; 1442 m | |
| **2** | *o*-TolSn(O$_2$CPy)$_3$·2H$_2$O | 1680 vs | 1340 vs | 340 | 1602 s; 1600 s; 1569 s; 1471 s; 1445 m | |
| **3** | *p*-ClPhSn(O$_2$CPy)$_3$·2H$_2$O | 1698 vs, 1680 vs | 1331 vs, 1400 s | 357, 280 | 1605 s; 1565 s; 1473 s; 1444 m | |
| **4** | *o*-ClPhSn(O$_2$CPy)$_3$·2H$_2$O | 1680 vs | 1332 vs | 348 | 1602 s; 1569 s; 1472 s; 1445 m | |
| **5** | *o*-ClBzSn(O$_2$Cpy)$_3$·2H$_2$O | 1681 vs | 1338 vs | 343 | 1602 s; 1569 s; 1471 s; 1441 m; 1439 m | |
| (II) | RSn(Ox)$_3$ | | | | | |
| | | ν(C–N) (cm$^{-1}$) | ν(C–O) (cm$^{-1}$) | ν(Sn–C) (cm$^{-1}$) | ν(Sn–O) (cm$^{-1}$) | ν(Sn–N) (cm$^{-1}$) |
| **6** | PhSn(Ox)$_3$ | 1570 s | 1105 s | 565 w | 510 s | 395 m |
| **7** | *p*-TolSn(Ox)$_3$ | 1570 s | 1115 m, 1105 s | 565 w, 575 w | 510 s | 400 m, 390 w |
| **8** | *o*-TolSn(Ox)$_3$ | 1570 s | 1115 m, 1105 s | 570 w | 510 s | 400 m |
| **9** | *p*-ClPhSn(Ox)$_3$ | 1570 s | 1115 m, 1105 s | 565 w | 515 s | 400 m, 390 w |
| **10** | *o*-ClPhSn(Ox)$_3$ | 1570 s | 1110 s | 565 vw | 515 s | 395 m |
| **11** | *o*-ClBzSn(Ox)$_3$·CHCl$_3$ | 1570 s | 1110 s | 570 vw | 525 s | 400 m |

[a] See Table 1 and Fig. 1. Abbreviations: s = strong; m = medium; w = weak; v = very. Solid compounds in KBr pellets. Numbers **1**–**5**: a large band around 3400 cm$^{-1}$ is attributed to H$_2$O vibrations.

Table 8
$^1$H-NMR spectral data [$\delta$ (ppm) with respect to TMS] for mono-organotin(IV) derivatives of pyridine-2-carboxylic acid and 8- hydroxyquinoline in $CDCl_3$ solutions

| Number | Compound [a] | H-3 [b] | H-4 [b] | H-5 [b] | H-6 [b] | *R* [c] |
|---|---|---|---|---|---|---|
| (I) | $HO_2CPy$ and $RSn(O_2CPy)_3{\cdot}2H_2O$ | | | | | |
| | $HO_2CPy$ [d] | 8.17 | 8.08 | 7.70 | 8.81 | – |
| **1** | *p*-TolSn$(O_2CPy)_3{\cdot}2H_2O$ | 8.40 d | 8.11 t | 7.69 t | 8.87 b | 7.62 d; 7.16 d; 2.29 s |
| **2** | *o*-TolSn$(O_2CPy)_3{\cdot}2H_2O$ | 8.33 d | 8.08 t | 7.69 t | 9.10 b | 7.23–6.93 m; 2.61 s |
| **3** | *p*-ClPhSn$(O_2CPy)_3{\cdot}2H_2O$ | 8.42 d | 8.12 t | 7.71 t | 8.89 b | 7.69 d; 7.32 d |
| **4** | *o*-ClPhSn$(O_2CPy)_3{\cdot}2H_2O$ | 8.38 d | 8.14 t | 7.72 t | 9.06 b | 7.93–7.72 m; 7.22–7.00 m |
| **5** | *o*-ClBzSn$(O_2Cpy)_3{\cdot}2H_2O$ | 8.28 d | 8.05 t | 7.64 t | 8.99 b | 7.08–7.00 m; 6.96–6.68 m; 3.29 s [e] |
| **5′** | BzSn$(O_2CPy)_3$ [g] | 8.29 d | 8.08 t | 7.68 t | 8.92 b | 7.26–7.05 m; 6.95–6.65 m; 3.15 s [f] |
| (II) | HOx and RSn(Ox)$_3$ | | | | | |
| | | H-2 [b] | H-4 [b] | R [c] | | |
| | HOx [h] | 8.79 d | 8.12 d | – | | |
| **6** | PhSn(Ox)$_3$ | 9.03 d; 8.79 d | 8.17 d; 8.06 d | 7.52–7.11 m | | |
| **7** | *p*-TolSn(Ox)$_3$ | 9.01 d; 8.78 d | 8.16 d; 8.04 d | 7.51–7.11 m; 2.14 s | | |
| **8** | *o*-TolSn(Ox)$_3$ | 9.12 d; 8.78 d | 8.16 d; 7.79 d | 7.51–7.05 m; 2.76 s (12 Hz) | | |
| **9** | *p*-ClPhSn(Ox)$_3$ | 9.01 d; 8.76 d | 8.14 d; 8.02 d | 7.48–7.06 m | | |
| **10** | *o*-ClPhSn(Ox)$_3$ | 8.79 d | 8.17 d | 7.48–7.22 m | | |
| **11** | *o*-ClBzSn(Ox)$_3{\cdot}CHCl_3$ | 8.99 d; 8.76 d | 8.13 d; 7.97 d | 7.48–7.14 m; 3.11 s | | |

[a] See Table 1. Abbreviations: s = singlet; d = doublet; t = triplet; m = multiplet; b = broad.
[b] Numbering of protons in the ligand, see Fig. 1A and B.
[c] $\delta$ of protons in the organic group bound to Sn; see Fig. 1C.
[d] Ref. [82].
[e] Coupling constants $^2J(^{119}Sn^1H)$: 167 Hz.
[f] Coupling constants $^2J(^{119}Sn^1H)$: 160 Hz.
[g] Mixture with the complex of BzHg$^{II}$, see Sections 2 and 2.2.
[h] Ref. [19b].

and the resonance of ligand H-4 goes gradually downfield with increasing N → Sn interaction [44]. Downfield shifts of ligand $\delta$ ($^1$H) then generally indicate a greater extent of Ox$^-$–Sn chelation [34]. Analogous criteria have been reported for LC-2 and LC-8 [55]. For example, $\delta$ (H-2) shifts upfield, and $\delta$ (H-4) downfield, in $^n$BuSn(Ox)$_3$, (*p*-Tolyl)$_2$Sn(Ox)$_2$ and $(C_6F_5)_2$Sn(Ox)$_2$ with respect to HOx [19b,43] which is attributed to N → Sn coordination with the consequent deshielding of H-2; in fact, H-2 in HOx appears to be shielded by the lone electron pair of the N atom [44,50,54].

In the RSn(Ox)$_3$ complexes Numbers **6**–**9** and **11**, Table 8(II), two sets of $\delta$ ($^1$H) signals have been detected, which is interpreted in terms of the occurrence of two different types of Ox$^-$ coordination to RSn$^{IV}$. The latter is in line with the crystal and molecular structure of *p*-ClPhSn(Ox)$_3$, where two different sets of N–Sn bond lenghts (one shorter and two longer bonds) have been detected (vide supra: Table 3 and Fig. 2). The same holds for the $CDCl_3$ solutions, as extracted from the integration of the $\delta$ (H-2) and $\delta$ (H-4) signals; in fact, for *p*-ClPhSn(Ox)$_3$ the ratio 2:1 has been detected for the ('weak') coordination at 9.01 and 8.02 ppm with respect to the ('strong') coordination at 8.76 and 8.14 ppm (Table 8(II)), the same occurring also for complexes **7**, **8**, **11**, R being *p*-Tolyl, *o*-Tolyl and *o*-ClBz. Instead, the ratio is reversed in PhSn(Ox)$_3$, Number **6**; moreover, in *o*-ClPhSn(Ox)$_3$, Number **10**, a single set of $\delta$ ($^1$H) signals is detected, which would indicate the occurrence of three equivalent Ox$^-$ ligands with 'strong' tin coordination, according to findings for $^n$BuSn(Ox)$_3$ [43].

In the $^{13}$C-NMR spectra of the complexes RSn(Ox)$_3$, on the other hand, single signals are detected for $\delta$ ($^{13}$C) of the ligand atoms C-2 (adjacent to N) and C-8 (bound to O), Fig. 1 and Table 9(II), which would suggest the bonding equivalence of the three Ox$^-$ coordinated to Sn. Limited $\delta$ ($^{13}$C) shifts are detected, analogous to literature reports for a series of R$_n$Sn$^{IV}$ ($n = 2$, 3) coordinated by Ox$^-$ [50].

The order of magnitude of $\delta$ ($^{119}$Sn) chemical shifts for complexes **1**–**5′** and **7**–**11** in Table 10 indicates the occurrence of 7-coordinated tin centers, in line with parameters reported for a series of organotin(IV) com-

Table 9
$^{13}$C-NMR spectral data [$\delta$ (ppm) with respect to TMS] for mono-organotin(IV) derivatives of pyridine-2-carboxylic acid and 8-hydroxyquinoline in $CDCl_3$ solutions

| Number | Compound [a] | LC-2 [b] | LC-3 [b] | LC-4 [b] | LC-5 [b] | LC-6 [b] | LC = 0 [b] | C-1 [c] | C-7 [c]; C-8 [c] |
|---|---|---|---|---|---|---|---|---|---|
| (I) | $HO_2CPy$ and $RSn(O_2CPy)_3\cdot 2H_2O$ | | | | | | | | |
| | $HO_2CPy$ [d] | 148.4 | 124.8 | 137.6 | 127.2 | 149.5 | 166.2 | – | – |
| **1** | *p*-$TolSn(O_2CPy)_3\cdot 2H_2O$ | 146.4 | 125.2 | 140.9 | 127.2 | 146.4 | 165.2 | 146.1 | 21.0 |
| **2** | *o*-$TolSn(O_2CPy)_3\cdot 2H_2O$ | 146.7 | 124.9 | 141.6 | 127.9 | 146.7 | 163.9 | 146.2 | 24.0 |
| **3** | *p*-$ClPhSn(O_2CPy)_3\cdot 2H_2O$ | 146.6 | 125.5 | 141.1 | 128.0 | 146.7 | 165.2 | 146.2 | – |
| **4** | *o*-$ClPhSn(O_2CPy)_3\cdot 2H_2O$ | 146.9 | 124.7 | 141.6 | 127.6 | 146.9 | 163.7 | 146.2 | – |
| **5** | *o*-$ClBzSn(O_2CPy)_3\cdot 2H_2O$ | 146.6 | 124.9 | 141.4 | 127.7 | 146.6 | 164.1 | 146.2 | 33.8 |
| **5′** | $BzSn(O_2CPy)_3$ [e] | 146.9 | 125.0 | 141.2 | 127.8 | 146.9 | 164.2 | 146.2 | 35.8 |
| (II) | HOx and $RSn(Ox)_3$ | | | | | | | | |
| | | LC-2 [b] | LC-8 [b] | C-1 [c] | C-7; C-8 [c] | | | | |
| | HOx [g] | 147.4 | 152.6 | – | – | | | | |
| **7** | *p*-$TolSn(Ox)_3$ | 145.6 | 157.4 | 147.8 | 21.3 | | | | |
| **8** | *o*-$TolSn(Ox)_3$ | 145.7 | 156.9 | 147.8 | 23.8 | | | | |
| **9** | *p*-$ClPhSn(Ox)_3$ | 145.6 | 157.0 | 146.8 | – | | | | |
| **10** | *o*-$ClPhSn(Ox)_3$ | 145.8 | [f] | 147.8 | – | | | | |
| **11** | *o*-$ClBzSn(Ox)_3\cdot CHCl_3$ | 145.9 | 157.3 | 147.8 | 34.3 | | | | |

[a] See Table 1.

[b] Carbon atoms in the ligand. See Fig. 1.

[c] Carbon atoms in the radicals bound to Sn. See Fig. 1.

[d] Data from Ref. [83], DMSO solutions.

[e] Mixture with the complex of $BzHg^{II}$, see Section 2.2.

[f] Complex **6**, $PhSn(Ox)_3$, and LC-8 for complex **10**: data not measured owing to insufficient solubility.

[g] Data from Ref. [19b].

plexes [48]. For compounds $RSn(O_2CPy)_3\cdot 2H_2O$, seven coordination of Sn could be assumed to be due to bonding by the three carboxylate groups (monodentate), one ligand nitrogen, and the two $H_2O$ molecules; the latter in line with the magnitude of ligand $\delta$ ($^{1}$H) parameters for H-6, Table 8(I), discussed here in the preceding. As far as complexes $RSn(Ox)_3$ are concerned, seven coordination is also suggested by the value $\delta$ ($^{119}$Sn) $= -561$ ppm (vs. TMT) reported for $^{n}BuSn(Ox)_3$ [48,57].

## 4. UV–vis spectroscopy

The occurrence of metal chelation by N, O donor atoms in 8-hydroxyquinoline complexes has been succesfully inferred by electronic spectroscopy in solution phases since the early fifties [58], and the method has been widely employed for the study of solutions of organotin(IV) oxinates [33–39,43,45,50]: the occurrence of absorption bands with maxima in the range 360–400 nm corresponds to metal chelation, while bands around 315 nm (as the data for the free ligand) indicate oxygen–metal coordination only. In particular, $^{n}BuSn(Ox)_3$ in dry benzene shows a maximum at 385 nm with $\varepsilon = 2.5 \times \varepsilon(Me_3Sn(Ox))$ [43], which has been interpreted in terms of tin chelation by all three oxinate ligands, yielding a pentagonal bipyramidal tin coordination environment [43]. The spectra for $RSn(Ox)_3$ complexes **6**–**11** in $CHCl_3$ solutions show $\lambda_{max} = 380 \div 382$ nm, which indicates tin chelation by the three $Ox^-$ ligands, analogously to $^{n}BuSn(Ox)_3$ in benzene.

## 5. Conclusions

In the solid state, complexes $RSn(O_2CPy)_3\cdot 2H_2O$ and $RSn(Ox)_3$ exhibit a common pentagonal bipyramidal configuration, with 7-coordinated Sn, as extracted from

Table 10
$^{119}$Sn-NMR chemical shifts [$\delta$ (ppm) with respect to TMT] of mono-aryltin(IV) and mono-benzyltin(IV) complexes with pyridine-2-carboxylic acid and 8-hydroxyquinoline in $CDCl_3$ solutions

| Number | Compound [a] | $\delta$ (ppm) |
|---|---|---|
| **1** | *p*-$TolSn(O_2CPy)_3\cdot 2H_2O$ | −620 |
| **2** | *o*-$TolSn(O_2CPy)_3\cdot 2H_2O$ | −671 |
| **3** | *p*-$ClPhSn(O_2CPy)_3\cdot 2H_2O$ | −626 |
| **4** | *o*-$ClPhSn(O_2CPy)_3\cdot 2H_2O$ | −679 |
| **5** | *o*-$ClBzSn(O_2CPy)_3\cdot 2H_2O$ | −644 |
| **5′** | $BzSn(O_2CPy)_3$ [b] | −642 |
| **7** | *p*-$TolSn(Ox)_3$ | −611 |
| **8** | *o*-$TolSn(Ox)_3$ | −618 |
| **9** | *p*-$ClPhSn(Ox)_3$ | −615 |
| **10** | *o*-$ClPhSn(Ox)_3$ | −616 |
| **11** | *o*-$ClBzSn(Ox)_3\cdot CHCl_3$ | −593 |

[a] See Table 1. Complex **6**, $PhSn(Ox)_3$: data not measured owing to insufficient solubility.

[b] Mixture with the complex of $BzHg^{II}$, see Section 2.2.

X-ray diffractometry for *p*-ClPhSn(Ox)$_3$·2CHCl$_3$, as well as from $^{119}$Sn Mössbauer and vibrational spectroscopy. In RSn(O$_2$CPy)$_3$·2H$_2$O species, 7-coordinated Sn could arise from chelation by bidentate ligands (through O- and N- atoms) or by one chelating and two monodentate carboxylate groups and, in addition, two H$_2$O molecules to tin. In solution phases (CDCl$_3$ and CHCl$_3$), the same bonding and structure of the monomeric molecules would persist, according to $^1$H-, $^{13}$C- and $^{119}$Sn-NMR, and UV–vis, spectroscopic data, as well as to the determined molecular mass.

## 6. Supplementary material

Crystallographic data for the structural analyses have been deposited with the Cambridge Crystallographic Data Centre, CCDC NO. 114783 for p-ClPhSn(Ox)$_3$ (**9a**). Copies of this information may be obtained free of charge from The Director, CCDC, 12 Union Road, Cambridge CB2 1EZ, UK (Fax: +44-1223-336-033; e-mail: deposit@ccdc.cam.ac.uk or www: http://www.ccdc.ac.uk).

## References

[1] F. Huber, R. Schmiedgen, M. Schürmann, R. Barbieri, G. Ruisi, A. Silvestri, Appl. Organomet. Chem. 11 (1997) 869.

[2] See e.g. C. Wei, N.W. Kong, V.G. Kumar Das, G.B. Jameson, R.J. Butcher, Acta Crystallogr. 45 (1989) 861.

[3] I.W. Nowell, J.S. Brooks, G. Beech, R. Hill, J. Organomet. Chem. 244 (1983) 119.

[4] T.P. Lockhart, F. Davidson, Organometallics 6 (1987) 2471.

[5] D.V. Naik, C. Curran, Inorg. Chem. 10 (1971) 1017; id., V Int. Conf. Organomet. Chem. Moscow, August 16–21, 1971, Abstracts, Vol. I, com. 71, p. 185.

[6] P.G. Harrison, R.C. Phillips, J. Organomet. Chem. 99 (1975) 79.

[7] P.G. Harrison, R.C. Phillips, J. Organomet. Chem. 182 (1979) 37.

[8] L. Prasad, E.J. Gabe, F.E. Smith, Acta Crystallogr. B38 (1982) 1325.

[9] M.M. McGrady, R.S. Tobias, J. Am. Chem. Soc. 87 (1965) 1909.

[10] D.W. Allen, J.S. Brooks, R. Formstone, A.J. Crowe, P.J. Smith, J. Organomet. Chem. 156 (1978) 359.

[11] W.F. Howard, W.H. Nelson, J. Mol. Struct. 53 (1979) 165.

[12] A.J. Crowe, R. Hill, P.J. Smith, J.S. Brooks, R. Formstone, J. Organomet. Chem. 204 (1981) 47.

[13] W.F. Howard Jr., R.W. Crecely, W.H. Nelson, Inorg. Chem. 24 (1985) 2204.

[14] S. Dietzel, K. Jurkschat, A. Tzschach, A. Zschunke, Z. Anorg. Allg. Chem. 537 (1986) 163.

[15] E.O. Schlemper, Inorg. Chem. 6 (1967) 2012.

[16] V.G. Kumar Das, C. Wei, Y.C. Keong, E. Sinn, J. Chem. Soc. Chem. Comm. (1984) 1418.

[17] S.W. Ng, C. Wei, V.G. Kumar Das, J.P. Charland, F.E. Smith, J. Organomet. Chem. 364 (1989) 343.

[18] E. Kellö, V. Vrábel, J. Holecek, J. Sivý, J. Organomet. Chem. 493 (1995) 13.

[19] (a) M. Schürmann, Dissertation, University of Dortmund, Germany (1995). (b) K. Wolf, id. (1993).

[20] M.A. Mullins, C. Curran, Inorg. Chem. 7 (1968) 2584.

[21] R.C. Poller, J.N.R. Ruddick, J. Chem. Soc. A (1969) 2273.

[22] K.M. Ali, D. Cunningham, M.J. Frazer, J.D. Donaldson, B.J. Senior, J. Chem. Soc. A (1969) 2836.

[23] B.W. Fitzsimmons, N.J. Seeley, A.W. Smith, Chem. Comm. (1968) 390.

[24] B.W. Fitzsimmons, N.J. Seeley, A.W. Smith, J. Chem. Soc. A (1969) 143.

[25] A.G. Davies, L. Smith, P.J. Smith, J. Organomet. Chem. 23 (1970) 135.

[26] F.P. Mullins, Canad. J. Chem. 48 (1970) 1677.

[27] R.V. Parish, C.E. Johnson, J. Chem. Soc. A (1971) 1906.

[28] J.N.R. Ruddick, J.R. Sams, J. Chem. Soc. Dalton Trans. (1974) 470.

[29] T.K. Sham, G.M. Bancroft, Inorg. Chem. 14 (1975) 2281.

[30] S.N. Bhide, P. Umapathy, M.P. Gupta, D.N. Sen, J. Inorg. Nucl. Chem. 40 (1978) 1003.

[31] H. Negita, R. Boku, S. Ichiba, Bull. Chem. Soc. Japan 53 (1980) 537.

[32] K.D. Ghuge, P. Umapathy, M.P. Gupta, D.N. Sen, J. Inorg. Nucl. Chem. 43 (1981) 653.

[33] V.G. Kumar Das, S.W. Ng, J. Singh, P.J. Smith, R. Hill, J. Organomet. Chem. 214 (1981) 183.

[34] V.G. Kumar Das, S.W. Ng, P.J. Smith, Inorg. Chim. Acta 49 (1981) 149.

[35] T. Tanaka, M. Komura, Y. Kawasaki, R. Okawara, J. Organomet. Chem. 1 (1964) 484.

[36] R. Barbieri, G. Faraglia, M. Giustiniani, L. Roncucci, J. Inorg. Nucl. Chem. 26 (1964) 203.

[37] L. Roncucci, G. Faraglia, R. Barbieri, J. Organomet. Chem. 1 (1964) 427.

[38] G. Faraglia, L. Roncucci, R. Barbieri, Ric. Sci. 35 (IIA) (1965) 205.

[39] K. Kawakami, R. Okawara, J. Organomet. Chem. 6 (1966) 249.

[40] W. Kitching, J. Organomet. Chem. 6 (1966) 586.

[41] F. Huber, H.-J. Haupt, R. Kaiser, Proc. IX I.C.C.C., St. Moritz-Bad, September 5–9, 1966; p. 51.

[42] F. Huber, R. Kaiser, J. Organomet. Chem. 6 (1966) 126.

[43] K. Kawakami, Y. Kawasaki, R. Okawara, Bull. Chem. Soc. Japan 40 (1967) 2693.

[44] Y. Kawasaki, Organic Magn. Reson., 2 (1970) 165; and Refs. therein.

[45] C.D. Barsode, P. Umapathy, D.N. Sen, J. Indian Chem. Soc. 54 (1977) 1172.

[46] P.J. Smith, A.P. Tupciauskas, Annual Report NMR Spectrosc. 8 (1978) 271; and Refs. therein.

[47] J. Otera, J. Organomet. Chem. 221 (1981) 57.

[48] J. Otera, A. Kusaba, T. Hinoishi, Y. Kawasaki, J. Organomet. Chem. 228 (1982) 223.

[49] M. Nadvornik, J. Holecek, K. Handlir, A. Lycka, J. Organomet. Chem. 275 (1984) 43.

[50] V.K. Jain, J. Mason, B.S. Saraswat, R.C. Mehrotra, Polyhedron 4 (1985) 2089.

[51] A. Lycka, J. Holecek, M. Nadvornik, K. Handlir, J. Organomet. Chem. 280 (1985) 323.

[52] J. Holecek, M. Nadvornik, K. Handlir, A. Lycka, J. Organomet. Chem. 315 (1986) 299.

[53] S.J. Blunden, B.N. Patel, P.J. Smith, B. Sugavanam, Appl. Organomet. Chem. 1 (1987) 241.

[54] A. Lycka, J. Holecek, K. Handlir, Collect. Czech. Chem. Commun. 54 (1989) 2386.

[55] A. Lycka, J. Holecek, M. Nadvornik, Main Group Metal Chem. 12 (1989) 169; and Refs. therein.

[56] A. Lycka, J. Holecek, A. Sebald, I. Tkac, J. Organomet. Chem. 409 (1991) 331.

[57] V. Pejchal, J. Holecek, M. Nadvornik, A. Lycka, Collect. Czech. Chem. Commun. 60 (1995) 1492; and Refs. therein.

[58] (a) T. Moeller, A.J. Cohen, J. Am. Chem. Soc. 72 (1950) 3546. (b) T. Moeller, F.L. Pundsack, J. Am. Chem. Soc. 76 (1954) 617. (c) D. Blake, G.E. Coates, J.M. Tate, J. Chem. Soc. (1961) 756.

[59] D.D. Perrin, W.L.F. Armarego, Purification of Laboratory Chemicals, 3rd Ed., Oxford, 1988.

[60] K.A. Kozeschkow, Ber. Dtsch. Chem. Ges. 66 (1933) 1661.

[61] M. Dub, in Organometallic Compounds, R.W. Wein (Ed.), Compounds of Germanium, Tin and Lead, including Biological Activity and Commercial Application, Springer–Verlag, Berlin, 1967, Vol. II, 2nd ed, first supplement.

[62] G.M. Sheldrick, Acta Crystallogr. A46 (1990) 467.

[63] G.M. Sheldrick, SHELXL 93 — A Program for Crystal Structure Determination, University of Göttingen, Germany, 1993.

[64] J.A. Ibers, W.C. Hamilton (Eds.), International Tables for X-ray Crystallography, Vol. C, Kluwer Academic Publishers, Dordrecht, 1992.

[65] G.M. Sheldrick, SHELXTL Plus. Release 4.1, Siemens Analytical X-Ray Instruments Inc., 1991.

[66] R. Barbieri, M.T. Musmeci, J. Inorg. Biochem. 32 (1988) 89.

[67] R. Barbieri, G. Ruisi, A. Silvestri, A.M. Giuliani, A. Barbieri, G. Spina, F. Pieralli, F. Del Giallo, J. Chem. Soc. Dalton Trans. (1995) 467.

[68] R. Barbieri, F. Huber, L. Pellerito, G. Ruisi, A. Silvestri, in P.J. Smith (Ed.), Chemistry of Tin, Blackie Acad. and Prof., London, 1998; ch. 14, p. 496; and Refs. therein.

[69] J.N.R. Ruddick, Revs. Silicon, Germanium, Tin, Lead Compounds, 2 (1976) 115; Table 4D, p. 167.

[70] G.M. Bancroft, R.H. Platt, Adv. Inorg. Chem. Radiochem. 15 (1972) 59.

[71] G.M. Bancroft, V.G. Kumar Das, T.K. Sham, M.G. Clark, J. Chem. Soc. Dalton Trans. (1976) 643.

[72] R.V. Parish, in G.J. Long (Ed.), Mössbauer Spectroscopy Applied to Inorganic Chemistry, Vol. 1, Plenum Press, New York, 1984, p. 257.

[73] R. Barbieri, L. Pellerito, N. Bertazzi, G.C. Stocco, Inorg. Chim. Acta 11 (1974) 173.

[74] A. Barbieri, A.M. Giuliani, G. Ruisi, A. Silvestri, R. Barbieri, Z. Anorg. Allgm. Chem. 621 (1995) 89.

[75] R. Barbieri, A. Silvestri, F. Huber, C.-D. Hager, Can. J. Spectrosc. 26 (1981) 194.

[76] See e.g. R.S. Preston, in: G.K. Shenoy, F.E. Wagner (Eds.), Mössbauer Isomer Shifts, North Holland, Amsterdam, 1978, ch. 6a, p. 292.

[77] G.K. Shenoy, F.E. Wagner, G.M. Kalvius, in: G.K. Shenoy, F.E. Wagner (Eds.), Mössbauer Isomer Shifts, North Holland, Amsterdam, 1978, ch. 3, p. 101; P.A. Flinn, ibid., ch. 9a, p. 611.

[78] See e.g. H.A. Stöckler, H. Sano, in: I.J. Gruverman (Ed.), Mössbauer Effect Methodology, Plenum Press, New York, 1970, vol. 5, p. 3.

[79] M. Schürmann, F. Huber, Acta Crystallogr. C50 (1994) 206.

[80] R. Barbieri, F. Huber, G. Ruisi, A. Silvestri, unpublished results.

[81] M. Domagala, F. Huber, H. Preut, Z. Anorg. Allg. Chem. 582 (1990) 37.

[82] Nuclear Magnetic Resonance Standard Spectra, 14695 M, Sadtler Research Laboratories, Inc., 1973.

[83] G.I. Moore, A.R. Kirk, R.A. Newmark, J. Heterocycl. Chem. 16 (1979) 789.

[84] M. Schürmann, A. Silvestri, G. Ruisi, M.A. Girasolo, A. Barbieri Paulsen, F. Huber, R. Barbieri, J. Organomet. Chem., in press.